Evidence for the incoming-velocity effect on negative fluorine ions scattering from a highly-oriented-pyrolytic-graphite surface

Lin Chen, Bin Ding, Yuan Li, Shunli Qiu, Feifei Xiong, Hu Zhou, Yanling Guo,* and Ximeng Chen†
School of Nuclear Science and Technology, Lanzhou University, Lanzhou 730000, China
(Received 26 August 2013; published 17 October 2013)

Negative-ion fractions depending on incident energies and angles have been measured for keV-energy fluorine negative ions scattering on a graphite surface at a scattering angle of 38°. For specular scattering, the fraction increases monotonously with increasing incident energy. A specific feature is the nonmonotonic angular dependence of the fraction with the variation of incident angles. It strongly indicates the interaction-time-dependent electron transfer process. The incident-velocity effect has been taken into account to analyze the experimental results, in which an exponential scaling is found.

DOI: 10.1103/PhysRevA.88.044901 PACS number(s): 79.20.Rf, 34.35.+a, 68.49.Sf, 34.50.Fa

Charge transfer processes in ion surface scattering are important not only from a fundamental physical interest, but also for practical applications, i.e., low-energy ion spectroscopy and secondary ion mass spectrometry. The charge transfer processes studied in the past mainly involved the neutralization and negative-ion formation of positive projectiles scattering on metallic surfaces either in grazing-angle or in large-angle scattering configurations [1–4]. Resonant charge transfer (RCT) [3–5], Auger neutralization (AN) [6,7], and collective excitation of plasmons [8] are involved in these scattering processes. Among them, RCT is considered experimentally and theoretically to be much more efficient in negative-ion formation of keV-energy atoms or ions scattering from metal surfaces [1–3,9–11].

Negative-ion formation on metal surfaces involves a tunneling transition of an electron from occupied levels of the valence band to the anion level of the projectile. The latter one is downward shifted due to image potential effects [12]. Departing from the surface, the negative ion quickly decays via resonant ionization and becomes an atom. Thus the population of the affinity level depends on its width, the surface work function, and the interaction time that the particle spends near the surface where RCT processes occur.

As the simplest system, the formation of H^- ions on metallic surfaces has attracted much more attention in the past, experimentally and theoretically [13–17]. Besides hydrogen negative ions, other negative ions, i.e., C^- [16], O^- [18,19], F^- [3,20,21], Cl^- [21], have also been studied at the same time, although these systems are more complicated due to the multielectron aspects [20,22].

Most research on negative-ion formation has been confined to interactions between ions and metallic surfaces. However, negative-ion formation on a graphite surface, one of the fusion first wall materials, is by far a less studied system. Only a few investigations for hydrogen ions scattering on graphite surfaces exist in the literature [23–27]. High H^- yields (∼30%) of 400-eV H_2^+ impact were measured on a high-work-function polycrystalline graphite surface [23] and were not observed from a highly oriented pyrolytic graphite (HOPG) (∼1.4%) [24]. H^- fraction from HOPG is of the order of 15% reported by Goldberg *et al*. in the 2–8-keV energy range [26], and the fraction is higher than that obtained from Al with work function of 4.4 eV [15]. Esaulov's group also reported the exit-angle dependence of hydrogen negative-ion fraction varying in the 2.5%–10% range in grazing scattering from HOPG [27]. This high value surprisingly conflicts with our understanding, because the binding energy of H^- (∼0.75 eV) is much smaller than the work function of HOPG (∼4.6 eV), and the outer electron of the H^- ion has a strong tendency to irreversibly transit from the ion itself to the surface. Hence high work functions would be essential to obtain low negative-ion fractions. Much effort therefore should be devoted to understanding the formation of negative ions on graphite surfaces.

A number of these experiments mentioned above always study negative-ion conversion for incident positive ions where two-step electron-capture processes are assumed, and the final charge state basically depends on the outgoing path of the scattering process. However, it may be questionable at higher incident energies. In addition, neutralization to the excited state of the incident ions may interrupt the negative-ion formation, but it can be avoided by using neutrals and negative ions. Direct experimental studies using negative-ion beams are much scarcer because the negative-ion source is needed. As a result, some theoretical studies have to indirectly compare with the available experimental results by positive projectiles [9,10,28]. Compared to positive ions, negative ions present a much smaller number of bound states with smaller binding energies. Thus negative-ion scattering on metal surfaces constitutes a very attractive model system to study RCT processes, in particular, the electron loss process.

Recently, there has been an increased interest in the scattering of negative ions from surfaces [29,30]. F^- fraction (∼1%) as a function of azimuthal angle for 3–4-keV F^- projectiles in grazing scattering on Au(110) was partially reported [30]. However, more work needs to be done with related investigations for some tens of keV energies. These studies motivated our present work. We measured the negative-ion fraction for 12.5–22.5-keV fluorine negative ions scattering on a HOPG surface. The maximum value of about 5% is slightly higher on a HOPG surface than on a Au(110) surface [30]. The negative-ion fraction is found to obey an exponential

*Corresponding author: guoyanling@lzu.edu.cn
†Corresponding author: chenxm@lzu.edu.cn

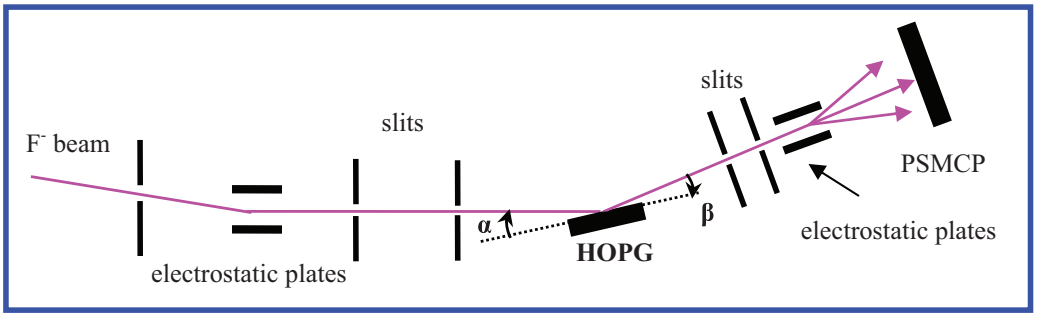

FIG. 1. (Color online) Schematic diagram of the experimental setup (not drawn to scale).

dependence on the inverse of the normal velocity component of the projectiles. In addition, the incident-angle dependence is explained in terms of the velocity effect related to the complete scattering trajectory.

The experiment was performed using the Lanzhou University cesium sputter negative-ion source. Negative fluorine ions were produced in source with energies from 12.5 up to 22.5 keV. The experimental setup is shown in Fig. 1. The negative-ion beam was collimated to a diameter of 3 mm by two slits 52.7 cm apart. A pair of electrostatic plates placed between these two slits separates the negative component from neutrals and steers the beams to pass through the third set of 2×2 mm^2 collimators 30.5 cm downstream of the second slit before entering an ultrahigh-vacuum (UHV) chamber, with a typical pressure of better than 3×10^{-7} Pa. The angular divergence of the primary beam was less than 0.28° [full width at half maximum (FWHM)] for all measurements. A HOPG surface was used as a target placed on a precise manipulator in the UHV chamber. The manufacturer quoted a mosaicity of less than 0.8°. The absence of oxidation layers and extremely low adsorption coefficient of compounds on the surface ensure cleanliness. To obtain an atomically flat surface, the layered structure of the graphite surface simplified the preparation procedure by removing several top layers with adhesive tape. The fresh surface was then transferred immediately to the vacuum and was prepared by cycles of annealing at about 773 K for 30 min. The scattering angle was fixed at 38°, and the incident angle α measured with respect to the surface plane was varied from 7° to 29°. The exit angle $\beta = (38° – \alpha)$. The reflected beam from the surface passed through the two post-target separated sets with 1×2 mm^2 apertures to avoid particle scattering on the tube wall. The charge states of scattered particles were then analyzed by a parallel-plate electrostatic deflector. A one-dimensional position sensitive microchannel plate (PSMCP) detector was located 60 cm downstream of the deflector.

The fraction of negative ions (neutrals) is defined as $N(\mathrm{F}^{-/0})/N(\mathrm{total})$ where $N(\mathrm{total})$ is the total number of scattered particles neglecting the recoiled carbon. The data were reproduced via a series of measurements made on different days. The experimental error in the fraction mainly determined by counting statistics, is less than 10% and no error bars are added in the following figures.

In Fig. 2(a) we show the negative-ion fraction as a function of incident angle for 22.5-keV negative fluorine ions scattering on a HOPG surface. It is found that the fraction first increases to about 5% with increasing incident angle, and then decreases as incident angle increases. Furthermore, the maximum value of the fraction generally corresponds to specular scattering and the shape in both sides is almost symmetrical. For low incident energies we investigated, this bell shape was also observed (not shown here). In contrast, the neutral fraction is large and first decreases and then increases with increasing incident angle. Figure 2(b) shows the negative-ion fraction measured for incident energies from 12.5 to 22.5 keV for two different incident angles. The results increase monotonously with increasing incident energy. The fraction corresponding to specular scattering (19°/19°) is always larger than that for the grazing incident angle (7°/31°) over the whole incident-energy range. In addition, the data shown in Fig. 2 are very similar to those scattering on silicon surfaces [31].

Let us first consider general features of negative-ion formation as mentioned in the Introduction. The affinity level of F^- is shifted down by the image potential and will cross and lie below the Fermi level of HOPG at a large distance of the order of 7 a.u. from the image plane. When the F^- ion moves away from the surface at distances larger than 7 a.u., one would expect resonant electron loss to occur more efficiently. Therefore, the long interaction time corresponding to decreasing the perpendicular velocity of scattered ions will favor electron loss near the surface in the coupling regime. As shown in Fig. 2, the negative-ion fraction decreases when the incident angle is larger than 19°, which is consistent with the previous results [15,18] due to the long interaction time with the surface. However, it is surprising that the fraction decreases with decreasing the incident angle (<19°), since the perpendicular velocity keeps growing, which would cause a higher negative-ion fraction. Thus it is difficult to understand this bell shape of the negative-ion fraction with the conventional "standard" picture. To the best of our knowledge, this bell shape has only been observed for 3–4-keV F atoms scattering on Ag, in which the F^- fraction is high, up to 60% [21], but the F^- fraction decreases with the increase of incident energies from 0.5 to 4 keV which is not consistent with our data.

For negative-ion formation, when positive ions scatter on metal surfaces, the complete neutralization occurring in the incoming path is an essential prerequisite. This is correct since the energy width usually becomes so large close to the surface that the memory effect concerning the initial

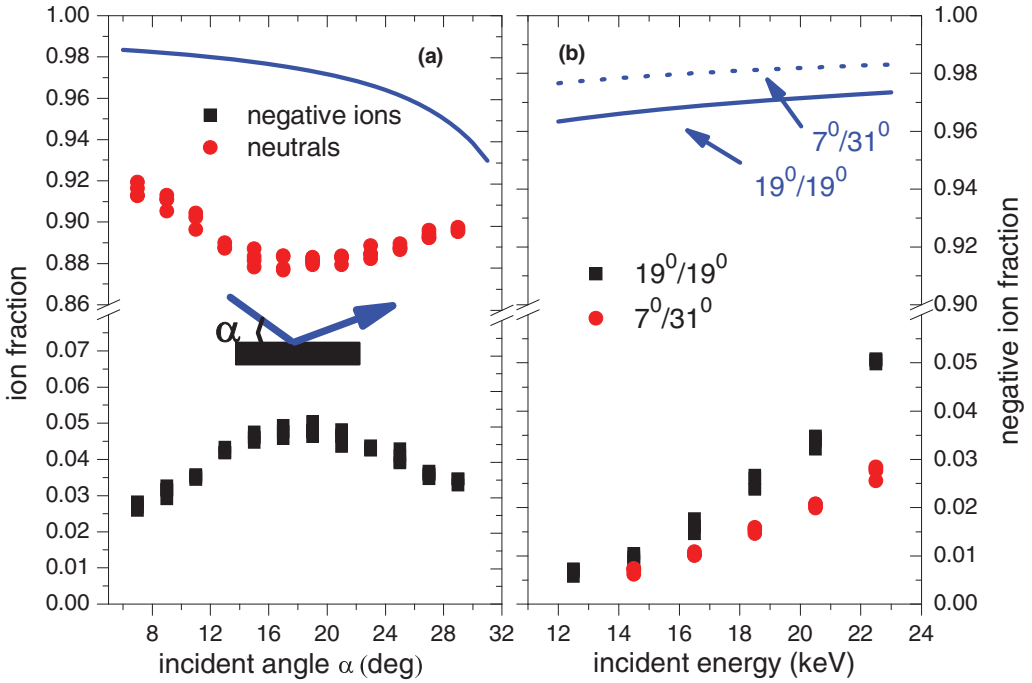

FIG. 2. (Color online) (a) Negative-ion fraction and neutral fraction as a function of incident angle with respect to the surface plane are measured for 22.5-keV F^- scattering on HOPG. The solid line is the calculated result from a rate-equation approach (see text). Inset shows the scattering geometry. (b) Negative-ion fraction as a function of incident energy is measured for different scattering configurations. The lines are calculated results.

charge state of the projectile is completely lost. As a consequence, it is reasonable to describe RCT processes only along the outgoing trajectory. In the limit of zero substrate temperature, the expression for negative-ion fraction $p^-_{\rm out} = \exp[-\frac{1}{v_{\perp \rm out}}\int_{z_0}^{\infty}\Gamma(z)dz]$ is in good agreement with experiment [15,17,22,32]. Here, $\Gamma(z)$ is the total transition probability, and $v_{\perp \rm out}$ is the velocity perpendicular component of the scattered ions. We also compared our results with a calculation using a rate-equation approach, in which the multielectron nature of processes and widths of the F^- affinity level for the jellium case were taken into account except for the parallel velocity effects [22]. The starting point of the trajectory integration was 3 a.u. measured from the image plane, smaller than the crossing distance (6.6–6.7 a.u.). It means that the F^- affinity level lies well below the Fermi level of the surface, and hence the capture occurring with unit probability is assumed. If the parallel velocity effects are included in the calculation, the negative-ion fraction would be significantly affected by changing the starting point and the work function of the surface. As shown in Fig. 2, the significant difference between experiment and model calculations indicates that both the details of the electronic structure of the surface and the coupling with other reaction channels should be considered for the nonmonotonic angular dependences of the negative-ion and neutral fractions, as well as electron correlation effects of the negative projectiles. Further quantitative calculation is beyond the scope of this work.

On the other hand, if we consider the data of neutrals, we can find that for small incident angles negative ions spend more time near the surface in the incoming path leading to forming more neutrals. In this respect, the incoming-velocity effect may be taken into account to understand our data. We intuitively divide the total scattering trajectory into three parts: incoming path, close collision, and outgoing path, where the part of close collision can be reasonably neglected because multiple collisions are important for the glancing incidence scattering [33]. Then the negative-ion fraction can be expressed by

$$p^- = p^-_{\rm in}p^-_{\rm out} \propto \exp\left[-v_0\left(\frac{1}{v\sin\alpha}+\frac{1}{v\sin\beta}\right)\right] = \exp\left[-v_0\left(\frac{1}{v_{\rm in}}+\frac{1}{v_{\rm out}}\right)\right], \quad (1)$$

where $p^-_{\rm in}$ and $p^-_{\rm out}$ are the formation (or survival) probability on the incoming and outgoing path respectively, which is similar to the formula described in the above paragraph. Here, $v_0 = \int_{z_0}^{\infty}\Gamma(z)dz$, the nuclear-energy loss is negligible, and v is the incident velocity in atomic units.

In Figs. 3 and 4 the negative-ion fractions are displayed in a semilogarithmic plot as a function of $\frac{1}{v_{\rm in}}+\frac{1}{v_{\rm out}}$. The data are well described by Eq. (1) with $v_0 = 0.76\times10^5$ m/s in Fig. 3, with 0.52×10^6 and 0.27×10^6 m/s in Fig. 4 for specular scattering and grazing incidence (7°), respectively. It strongly indicates the dynamical RCT processes, where the effective interaction time associated with $\frac{1}{v_{\rm in}}+\frac{1}{v_{\rm out}}$ plays an important role. From the experimental data, we can find that electron detachment dominates the scattering process. It is reasonable to believe this fact: the more the effective interaction time near the surface, the higher the electron detachment probability. In

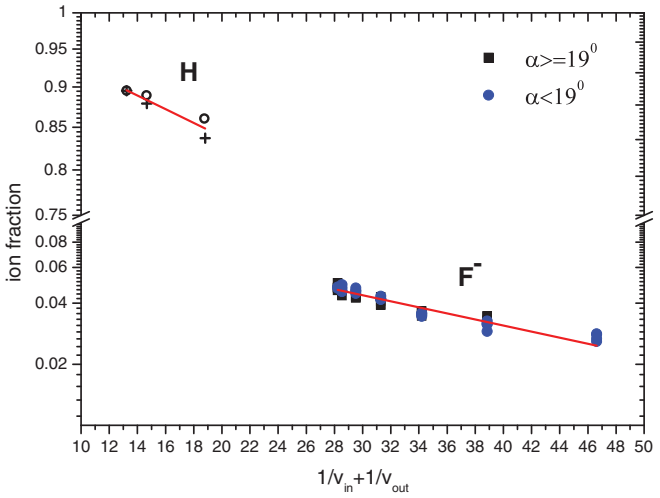

FIG. 3. (Color online) Logarithmic plot of negative-ion fraction for 22.5-keV F^- scattering on HOPG as a function of $\frac{1}{v_{in}} + \frac{1}{v_{out}}$. The data for incident angle of less than 19° are plotted with blue solid circles and for incident angle of larger than 19° with black solid squares. The straight line gives the best fitting with a slope of 0.76×10^5 m/s. The neutral fraction of H^+ ions derived from [26] is also plotted here for comparison, where the crosses represent the data for incident angle larger than 22.5°and the open circles for incident angle less than 22.5°.

fact, a similar expression has been successfully employed to describe Auger neutralization on metal surfaces [34], but it is not the case in the RCT process presented here.

In Fig. 3 for 22.5-keV F^- incidence, the decrease of incident angles from 19° to 7° corresponds to the increase of the effective interaction time, which leads to the low negative-ion fraction. This suggests that a majority of the long interaction time spent at more grazing incidence angles is in favor of getting a greater number of fluorine neutrals, so that there is not enough time left for neutrals to pick up electrons from

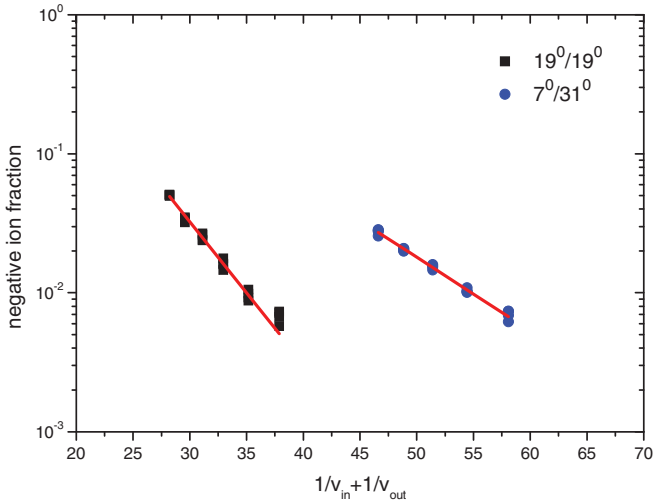

FIG. 4. (Color online) Logarithmic plot of negative-ion fraction as a function of $\frac{1}{v_{in}} + \frac{1}{v_{out}}$. The straight lines presenting the best fitting give a slope of 0.52×10^6 m/s for specular scattering and 0.27×10^6 m/s for the grazing incident angle of 7° and the exit angle of 31°.

the surface on the way out. At 19°, the negative-ion fraction is the highest, corresponding to the minimum of the effective interaction time. Beyond 19°, the interaction time increases again and causes the scattered negative ions to lose more electrons to the surface and finally the negative-ion fraction decreases. In order to explain our data, the incident path cannot be ignored. The data shown in Fig. 4 also support this conclusion: the shorter the effective interaction time, the higher the negative-ion fraction. The interaction time is longer for the grazing incidence (7°) than for specular scattering, which indicates the characteristic velocity v_0 is lower for 7° incidence, given the same incident energies. As the incident energy decreases, the negative-ion fraction trends down due to the long interaction time with the unoccupied conduction band.

In addition, the total ion fractions (positive and negative H ions) were reported by Bonetto *et al.* for 4-keV H^+ ions scattering on HOPG [26]. The total ion fraction first decreases and then increases with increasing the exit angle. Their calculated results only well reproduce the data at large exit angles and fail at low exit angles. The neutral fraction can be simply derived from their experimental data and is plotted in Fig. 3 for comparison. The neutral fraction presents a similar shape as our negative-ion fraction and can be well described by this exponential scaling. It suggests that the incident-velocity effect plays an important role in RCT, in particular for projectiles with relatively high energies and for specific collision configurations. The initial charge state of the projectile may affect the charge transfer process and the final ion fraction.

In summary, we measured the negative-ion fraction for 12.5–22.5-keV fluorine negative ions scattering on a HOPG surface. The fraction increases with increasing incident energy, but it is not the case for the incident-angle dependence of the fraction. The nonmonotonic angular dependence strongly indicates the dynamical electron transfer process. The experimental data obey well an exponential scaling. It indicates that the effective interaction time determines the negative-ion fraction so that the incoming-velocity or incident-trajectory effect should be taken into account. These findings are very different from previous results and are not consistent with the jellium model calculation using the rate-equation approach where only the outgoing trajectory is calculated. In this respect, other negative-ion scattering experiments are indeed required and are in progress in our group. We expect that this work will stimulate theoretical study on this subject.

The authors are grateful to Jinkun Liu, Yuguo Liu, Pengfei Li, Bin Du, Yan Zhang, Cong Wang, Yang Song, Zhaoxing Qiu, Binhai Pan, and Yunjun Hu for some help in the initial stage of this experiment; we thank Professor Jianxiong Shao for providing us with charge sensitive preamplifiers. This work was supported by the National Natural Science Foundation of China (Grants No. 11104124 and No. 11175075), the Fundamental Research Funds for the Central Universities (Grant No. lzujbky-2013-4), and the project sponsored by SRF for ROCS, SEM, and National Students' innovation and entrepreneurship training program (Grant No. 201210730073).

[1] T. Hecht, H. Winter, A. G. Borisov, J. P. Gauyacq, and A. K. Kazansky, Phys. Rev. Lett. **84**, 2517 (2000).
[2] A. G. Borisov, A. Mertens, S. Wethekam, and H. Winter, Phys. Rev. A **68**, 012901 (2003).
[3] L. Guillemot and V. A. Esaulov, Phys. Rev. Lett. **82**, 4552 (1999).
[4] C. Meyer, F. Bonetto, R. Vidal, E. A. García, C. Gonzalez, J. Ferrón, and E. C. Goldberg, Phys. Rev. A **86**, 032901 (2012).
[5] F. Bonetto, M. A. Romero, E. A. García, R. A. Vidal, J. Ferrón, and E. C. Goldberg, Phys. Rev. B **78**, 075422 (2008).
[6] A. Iglesias-García, E. A. García, and E. C. Goldberg, Phys. Rev. B **87**, 075434 (2013).
[7] T. Kravchuk, V. A. Esaulov, A. Hoffman, and R. C. Monreal, Nucl. Instrum. Methods Phys. Res., Sect. B **232**, 27 (2005).
[8] N. Lorente and R. Monreal, Phys. Rev. B **53**, 9622 (1996).
[9] A. G. Borisov, A. K. Kazansky, and J. P. Gauyacq, Phys. Rev. Lett. **80**, 1996 (1998); Phys. Rev. B **59**, 10935 (1999).
[10] H. Chakraborty, T. Niederhausen, and U. Thumm, Phys. Rev. A **70**, 052903 (2004).
[11] B. Obreshkov and U. Thumm, Phys. Rev. A **87**, 022903 (2013).
[12] H. Winter, Phys. Rep. **367**, 387 (2002).
[13] V. von Gemmingen and R. Sizmann, Surf. Sci. **114**, 445 (1982).
[14] F. Wyputta, R. Zimny, and H. Winter, Nucl. Instrum. Methods Phys. Res., Sect. B **58**, 379 (1991).
[15] M. Maazouz, A. G. Borisov, V. A. Esaulov, J. P. Gauyacq, L. Guillemot, S. Lacombe, and D. Teillet-Billy, Phys. Rev. B **55**, 13869 (1997).
[16] D. Teillet-Billy and J. P. Gauyacq, Surf. Sci. **239**, 343 (1990).
[17] A. G. Borisov, D. Teillet-Billy, and J. P. Gauyacq, Phys. Rev. Lett. **68**, 2842 (1992).
[18] M. Maazouz, L. Guillemot, T. Schlatholter, S. Ustaze, and V. A. Esaulov, Nucl. Instrum. Methods Phys. Res., Sect. B **125**, 283 (1997).
[19] C. Auth, H. Winter, A. G. Borisov, B. Bahrim, D. Teillet-Billy, and J. P. Gauyacq, Phys. Rev. B **57**, 12579 (1998).
[20] N. Lorente, A. G. Borisov, D. Teillet-Billy, and J. P. Gauyacq, Surf. Sci. **429**, 46 (1999).
[21] M. Maazouz, S. Ustaze, L. Guillemot, and V. A. Esaulov, Surf. Sci. **409**, 189 (1998).
[22] S. Ustaze, L. Guillemot, V. A. Esaulov, P. Nordlander, and D. C. Langreth, Surf. Sci. **415**, L1027 (1998).
[23] K. Tsumori, W. R. Koppers, R. M. A. Heeren, M. F. Kadodwala, J. H. M. Beijersbergen, and A. W. Kleyn, J. Appl. Phys. **81**, 6390 (1997).
[24] M. A. Gleeson and A. W. Kleyn, Nucl. Instrum. Methods Phys. Res., Sect. B **157**, 48 (1999).
[25] R. Souda, E. Asari, H. Kawanowa, T. Suzuki, and S. Otani, Surf. Sci. **421**, 89 (1999).
[26] F. Bonetto, M. A. Romero, E. A. Garcia, R. Vidal, J. Ferro, and E. C. Goldberg, Euro. Phys. Lett. **80**, 53002 (2007); R. A. Vidal, F. Bonetto, J. Ferro, M. A. Romero, Evelina A. Garcia, and E. C. Goldberg, Surf. Sci. **605**, 18 (2011).
[27] D. Datta, J. Shen, and V. A. Esaulov, Nucl. Instrum. Methods Phys. Res., Sect. B (in press), doi: 10.1016/j.nimb.2013.04.089.
[28] H. Chakraborty, T. Niederhausen, and U. Thumm, Phys. Rev. A **69**, 052901 (2004).
[29] L. Chen, Y. Guo, J. Jia, H. Zhang, Y. Cui, J. Shao, Y. Yin, X. Qiu, X. Lv, G. Sun, J. Wang, Y. Chen, F. Xi, and X. Chen, Phys. Rev. A **84**, 032901 (2011).
[30] L. Chen, J. Shen, J. E. Valdés, P. Vargas, and V. A. Esaulov, Phys. Rev. A **83**, 032901 (2011).
[31] L. Chen, Y. Li, B. Ding, Y. Guo, and X. Chen (unpublished).
[32] R. Brako and D. M. Newns, Rep. Prog. Phys. **52**, 655 (1989).
[33] M. Hillenkamp, J. Pfister, M. M. Kappes, and R. P. Webb, J. Chem. Phys. **111**, 10303 (1999).
[34] M. Draxler, R. Gruber, H. H. Brongersma, and P. Bauer, Phys. Rev. Lett. **89**, 263201 (2002).